Phase modulation and far-field spatial patterns due to the transformational thermal-lens effect

Ting Chen,* Shou-Jong Sheih, and J. F. Scott
Department of Physics, University of Colorado, Boulder, Colorado 80309-0390
(Received 9 April 1990; revised manuscript received 30 July 1990)

In earlier work we have reported a thermal-lens effect that is opposite in sign from and much stronger than the well-known effect in fluids and isotropic solids: Very near the transformation temperature in crystals undergoing structural phase transitions, certain indices of refraction have temperature derivatives that are large and positive ($\simeq +10^{-1}$ K^{-1}), in contrast to the negative values of dn/dT that arise from thermal expansion in glasses or fluids. We evaluated the steady-state and time-dependent behavior of these effects in $Ba_2NaNb_5O_{15}$ near $T_c = 850$ K. In the present paper we extend these studies to examine the far-field spatial pattern produced by self-induced phase modulation. We also utilize the thermal-lens effect to investigate the critical behavior near the tricritical point of $Ba_2NaNb_5O_{15}$, and the critical exponent β is obtained as $\beta_c = 0.28 \pm 0.01$ and $\beta_a = 0.31 \pm 0.01$.

I. INTRODUCTION

The thermal-lens effect in isotropic materials such as glasses and fluids[1] is well understood as arising from thermal expansion of the illuminated medium and concomitant decrease in index of refraction, producing a negative (concave) lens with typical focal length of the order 100 cm at mW powers. In ferroelectric and other materials the thermo-optic effect may result in an analogous effect, but the induced lens can be positive. The latter has been observed in barium sodium niobate by us[2,3] and previously in doped strontium barium niobate by Seglins and Krumins and co-workers.[4,5] We have discovered[2] that this effect can become very strong in crystals near the temperature of their structural phase transformations (e.g., the Curie temperature in ferroelectrics) which we term the "transformational thermal-lens effect." This thermal focusing arises from the fact that the temperature derivative of at least one index of refraction may be very large and positive as $T \rightarrow T_c$ from below, producing a positive (convex) thermal lens of very short focal length, $\simeq 3$ cm. In a second paper[3] we showed that the critical exponent β that describes the coexistence curve [that is, polarization P varies as ϵ^{β}, where ϵ is reduced temperature $(T_c - T)/T_c$] could be evaluated accurately from such thermal focusing data, obtaining a mean-field result $\beta \approx \frac{1}{4}$ for $Ba_2NaNb_5O_{15}$.

The basic ring structure of laser beams passing through nonlinear media has been noted by a number of investigators.[6-12] At modest cw powers the steady-state spatial pattern is quite similar to the interference observed in light trapped in filaments.[13] Several effects, both spatial and temporal, were observed in $Ba_2NaNb_5O_{15}$ to be very similar to those in fluids, including chirping above a power threshold $\simeq 1$ W.[2,3] In the present work we examine the detailed spatial steady-state structure of the far-field pattern due to thermal focusing near T_c in this crystal and give a quantitative comparison of theory and experiment.

II. THERMAL-LENS ABERRATION

When the self-focusing or defocusing of a laser beam passing through a medium is generated mainly by thermally induced refractive index change, the theoretical calculation can be carried out based on equations of heat transport. The radial intensity distribution of a Gaussian beam is

$$I \propto e^{-2(r/w_0)^2}, \tag{1}$$

where r is the distance from the axis of the beam and w_0 is the waist of the beam. In the case that thermal conduction dominates the heat dissipation, the steady-state heat equation of local heating yields the following expression for the radial temperature derivative:[1]

$$\frac{d\Delta T}{dr} = -\frac{0.12bP}{\pi k_T}\frac{1}{r}(1 - e^{-2(r/w_0)^2}), \tag{2}$$

where k_T is the thermal conductivity, b, the absorption coefficient, and P, the laser power inside the sample.

With a dimensionless variable $u = r/w_0$ and a boundary condition of $\Delta T = 0$ at $u = a$, when the axial attenuation of laser power is neglected, the local temperature increment is in an integral form:

$$\Delta T(u) = \frac{0.12bP}{\pi k_T}\int_a^u \frac{1}{u'}(1 - e^{-2(u')^2})du'. \tag{3}$$

The u-dependent part of this temperature distribution is an integral. For $a = 10$, a numerical calculation of this integral is plotted in Fig. 1 with a maximum value of 2.95. The index increment can be represented, in turn, as $\Delta n = (dn/dT)\Delta T$. Equation (3) can be written in the form of an exponential series. If we consider only the terms up to r^2 in the series, the refractive index has the form of $n = n_0[1 + \delta(r/w_0)^2]$, where δ is a numerical coefficient for the first term in a power series. In this situation the thermal lens is equivalent to a thin lens with a definite focal length. Such a treatment is called the para-

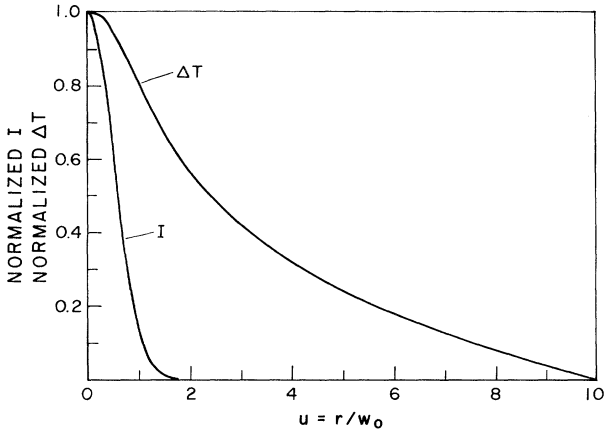

FIG. 1. Normalized radial distributions of Gaussian beam intensity $I(u)$ and of temperature increment $\Delta T(u)$.

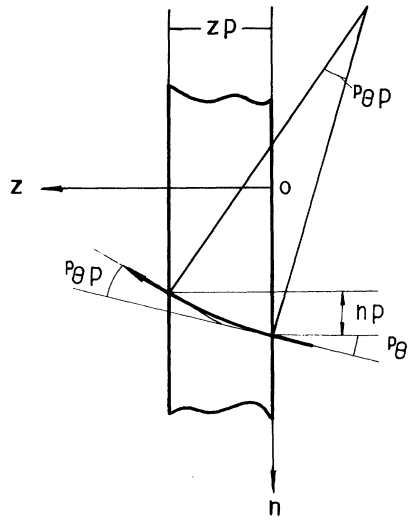

FIG. 2. Schematic illustration of light beam deflection in an inhomogeneous medium.

bolic approximation[1] and provides a general description of the thermal-lens effect.

Since the thermal-lens patterns generally present aberration, the simple thin-lens model is not sufficient for studying the details of the pattern. In principle, the ring pattern can be constructed from the diffraction theory of aberration. For greater accuracy, a comprehensive consideration of phase variation should include phase retardation at the input plane due to the curvature of the wave front of a Gaussian beam, the far-field Fresnel variation of phase, and the thermo-optic phase modulation.[7,11,14] Since we place the sample at the waist of the beam focused by a weakly convergent lens, the wave front at the input plane can be considered as planar and the divergence of the original beam is negligible. The far-field Fresnel diffraction is described by a Bessel function of zero order $J_0(k\theta r)$. Here k is the wave vector of the light, r, the distance from the illuminated axis, θ, the convergence angle. References 6 and 7 suggested that the thermal-lens pattern is dominated by an integral of this Bessel function. Our experiment shows that, as described below, the intensity distribution produced by the thermal lens appears at $k\theta r \sim 10^3$. This is far beyond the region where a Bessel function gives a distinct diffraction pattern. Our observation is not in a Bessel-function limit. A more mathematical comparison of the present work with Refs. 6 and 7 is given below in Appendixes A and B. In the following we start from the basic principle of light propagation in an inhomogeneous medium and then calculate the pattern induced by the self-phase modulation.

In a medium with inhomogeneous index distribution the radius of deflection for the curvature of the light beam, as shown in Fig. 2, is given by

$$\frac{1}{R}=\frac{1}{n}\frac{dn}{dr} . \tag{4}$$

The deflection angle is normally small. In reference to Eq. (2), it can be written as

$$\theta_d \approx \frac{L}{n}\frac{dn}{dr}=\frac{0.12bPL}{\pi k_T w_0 n}\frac{dn}{dT}\frac{1}{u}(1-e^{-2u^2}) , \tag{5}$$

where L is the sample thickness. The u-dependent part of Eq. (5) is $F(u)=(1-e^{-2u^2})/u$, which has the same normalized form as $\theta_d(u)$ and is plotted in Fig. 3. Because of the differential relation of Eq. (5) from Eq. (3), $F(u)_{\max}$ is related to the slope at the inflection point of the $\Delta T(u)$ curve and is found to be 0.9025 at $u=0.7926$.

The dependence of θ_d upon u means that for the part of beam of $u<0.79$, denoted as the "inner section" hereafter, the deflection angle increases with u, while for the part of $u>0.79$, denoted as the "outer section," it decreases with u. In other words, the distribution of beam intensity at any deflection angle is due to two contributions: that from the inner and outer sections of the illuminated part of the crystal. The superposition and interference of these two parts of the beam determine the thermal-lens pattern.

Although the basic concept of optical interference re-

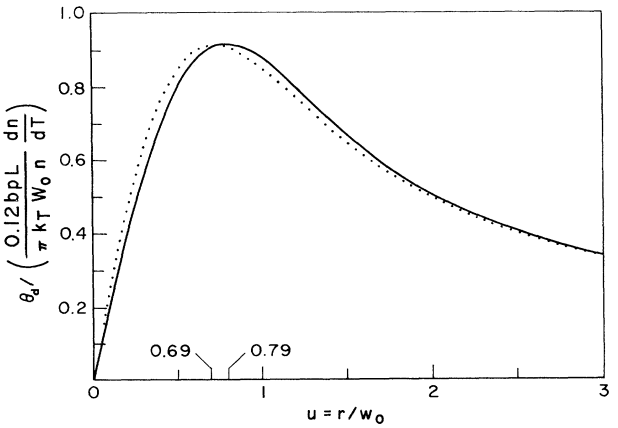

FIG. 3. Radial distribution of deflection angle θ_d (——), without beam deflection inside the sample and θ'_d (· · · ·), beam deflects continuously inside the sample.

quires spatial and temporal superposition of interfering waves, in order to make the calculation of the pattern tractable, we consider the interfering parts of the beam to be nearly parallel. This consideration is reasonable in a first approximation of the problem, because the intersection angles of the interfering parts are small (smaller than 4° in our experiment). Let u_1 and u_2 be the relative radial distances of the inner and outer sections of beam which deflect at the same angle. Their phase difference is

$$\Delta\phi=\phi_1-\phi_2=\frac{2\pi}{\lambda}[\Delta n(u_1)-\Delta n(u_2)] . \tag{6}$$

From $\Delta n=(dn/dT)\Delta T$ as well as Eqs. (3) and (5), it is found that for the calculation of $\Delta\phi$ only measured values of θ (maximum deflection angle, or beam convergence angle), w_0, and n are needed, while other parameters, such as b, P, L, k_T can be eliminated. Through the inverse function $u(\theta_d)$, the calculated $\phi_1(\theta_d)$, $\phi_2(\theta_d)$, and $\Delta\phi(\theta_d)$, are plotted in Fig. 4. The intensity attenuations occur at $\Delta\phi=(2n+1)\pi$, $n=0,1,2,\ldots$ and result in the ring pattern. According to the general two-beam interference theory and the relations of $E(\theta_d)$, $u(\theta_d)$, and $\Delta\phi(\theta_d)$, for a 200-point sampling, which corresponds to the resolution of our image processing system, a numerical analysis of the interference intensity $I(\theta_d)$ is obtained as Fig. 5. Since $\Delta\phi$ increases nonlinearly with decreasing reflection angle, the ring structure appears clearly only for thinner samples and in the outer part of pattern. In the center of the pattern the phase difference is, in fact, the phase modulation of the inner section alone. This plot gives three of the basic characteristics of the thermal-lens patterns: ring structure, limited size, and bright contour. The obvious contour provides a convenient definition of the pattern size, from which the beam convergence angle θ can be obtained easily.

In the above calculations the path length of the beam inside the sample is taken as L; this implies that the beam does not deflect inside the sample. In our detailed computer simulation, in which the sample is composed of a series of slices with a thickness of dz for each, for the light beam passing through each slice the increments in deflection angle and in radial displacement are

$$d\theta_d=\frac{dz}{w_0}\frac{1}{n}\frac{dn}{dT}\frac{d\Delta T}{du} , \tag{7}$$

$$du=\frac{dz}{w_0}\left[\theta_d+\frac{d\theta_d}{2}\right] . \tag{8}$$

Using the parameters indicated in Sec. IV of the present paper and matching the observed maximum deflection angle, this simulation gives a calculated beam path in the sample, as illustrated in Fig. 6. The corresponding deflection angle distribution is also shown in Fig. 3, in which the location of maximum θ_d moves down from $u=0.79$ to 0.69. The calculated phase modulations according to Eqs. (7) and (8) as well as the intensity distribution from the new set of $E'(\theta_d)$, $u'(\theta_d)$, and $\Delta\phi'(\theta_d)$ are very close to that shown in Figs. 4 and 5.

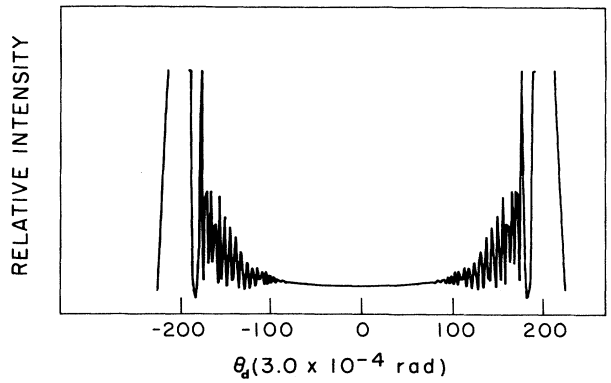

FIG. 5. Theoretical calculation of intensity distribution of thermal-lens pattern near T_c; no beam deflection inside the sample is supposed.

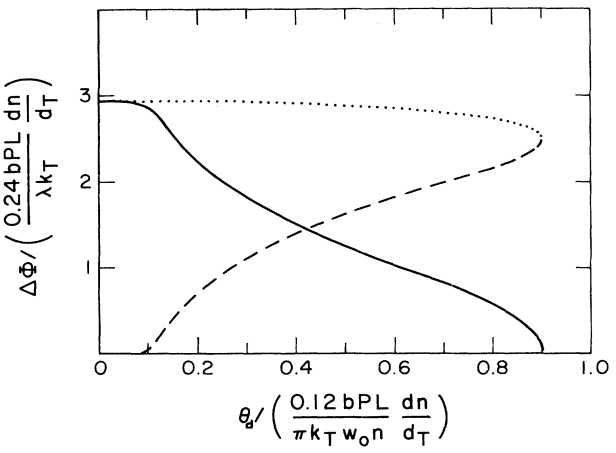

FIG. 4. Self-phase modulation of thermal lens: ϕ_1 (· · · ·), inner section of beam, $u<0.79$; ϕ_2 (— — —), outer section of beam, $u>0.79$; phase difference $\Delta\phi$ (——).

III. ELECTRO-OPTIC AND ELASTO-OPTIC COUPLING IN THE TRANSFORMATIONAL THERMAL-LENS EFFECT

The ferroelectric phase transition in tungsten-bronze–type $Ba_2NaNb_5O_{15}$ occurs at 560–585 °C depending on the slight stoichiometric variations during crystal growth. The structural transition of paraelectric $4/mmm(D_{4h}^5)$ to ferroelectric $4mm(C_{4v}^2)$ is characterized by the spontaneous polarization P_s along the crystal c axis. Yamada, Iwasaki, and Niizeki[15] and Singh, Draegert, and Geusic[16] have reported their measurements on optical properties in $Ba_2NaNb_5O_{15}$. Their results revealed that n_c increases with large slope as T_c is approached from below, while n_a and n_b are almost temperature independent. According to Eqs. (5) and (7), the temperature dependence of the beam convergence angle θ owing to the thermal-lens effect is mainly related to the

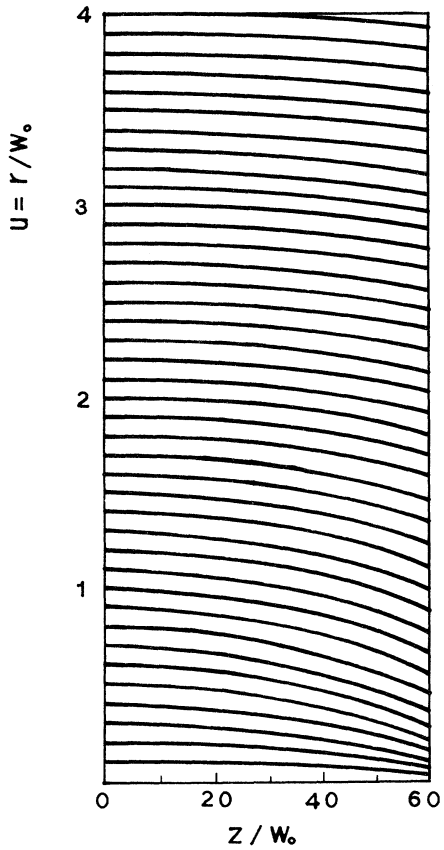

FIG. 6. Computer simulation of beam deflection inside the sample. The parameter dn/dT is selected to match the real beam divergence angle. Because of the different scales in abscissa and ordinate the deflection angle illustrated in this figure is exaggerated.

temperature behavior of dn/dT. The temperature behavior of n_c can be neglected, because it varies $<1\%$ in the temperature interval we are interested in; however, dn_c/dT can still be large very near T_c.

For oxygen-octahedra ferroelectrics, in the regime of linear optics, the index change of a mechanically and electrically free crystal is mainly because of the spontaneous polarization-optic effect. Among other possible origins, the thermal-expansion-induced birefringence is small in the temperature region we are interested in ($Ba_2NaNb_5O_{15}$'s dilatation constant is $\sim 10^{-3}$).[17] The ferroelectric phase transition in $Ba_2NaNb_5O_{15}$ is nonferroelastic, so that the strain-induced effect is not large. In this respect, $Ba_2NaNb_5O_{15}$ is different from the ferroelastic crystal As_2O_5, in which the change in optic birefringence is attributed to the elasto-optic coupling.[18] $Ba_2NaNb_5O_{15}$ belongs to the oxygen-octahedra ferroelectrics with a fourfold axis and an inversion center in paraelectric phase. Based on a free-energy expansion of Landau theory, the polarization's contribution to optical birefringence is given by DiDomenico and Wemple as[19]

$$\Delta n_c = -\tfrac{1}{2} n_c^3 (g_{11} - g_{12}) P_s^2 \ ; \tag{9}$$

here g_{11} and g_{12} are quadratic electro-optic coefficients and were proved to be only weakly temperature dependent. For pure electro-optic coupling Eq. (9) predicts, with Eqs. (5) and (7),

$$\theta(T) \sim \epsilon^{2\beta-1} \ . \tag{10}$$

Singh, Draegert, and Geusic[16] showed that T_c in $Ba_2NaNb_5O_{15}$ is near a tricritical point, so $\beta \cong \frac{1}{4}$. Hence, it is predicted that

$$\theta(T) \sim \epsilon^{-1/2} \ , \tag{11}$$

where ϵ is reduced temperature $(T_c - T)/T_c$.

IV. EXPERIMENTAL RESULTS AND DISCUSSIONS

The experiment setup has been reported previously.[2] $Ba_2NaNb_5O_{15}$ samples were prepared in a or b cut. A typical sample size is $1.3 \times 4 \times 6$ mm^3. The single ferroelectric domain is obtained by means of a poling process with an applied field of 350 V/cm during cooling from 600 °C to lower temperature. Because the measurements are performed far above the ferroelastic transition temperature around 300 °C, a detwinning process is not necessary. The sample was placed in an oven with temperature control accuracy of ± 0.1 °C. The temperature was measured by a thermocouple attached to the sample holder. The output 514.5 nm excitation of an Ar^+ laser was focused weakly onto the sample with the light polarization parallel to the crystal c axis. The laser power at the sample was 0.33 W. The Gaussian beam waist at the focusing point, where the sample was placed, was $w_0 = 0.213$ mm. The pattern's full size d was measured on a screen, 204.5 cm from the sample, manually or through a video-camera–computer on-line system. An image processing program was used to obtain pattern parameters. Because the focal length of our thermal lens ($\simeq 3$ cm) is much shorter than the observation distance z, the beam convergence angle in Eqs. (10) and (11) can be considered as equal to the measured divergence angle $\theta = d/2z$. It is observed that the pattern's structure remains unchanged when the observation plane is moved from the location directly outside the oven to a few meters away. This verifies that only thermal-induced phase modulation is important for the formation of the patterns and that Fresnel diffraction can be ignored.

A typical thermal-lens pattern near T_c is shown in Fig. 7. After passing through T_c by heating, the pattern shrinks rapidly. The beam divergence angle at T_c is 4.3°. For $Ba_2NaNb_5O_{15}$ the following parameters are used: $b = 0.257$ cm^{-1},[20] $k_T = 0.059$ W/cm K,[20] $n_c = 2.33$.[16] According to Eq. (5) and the observed divergence angle, the temperature gradient of the diffractive index at T_c is obtained as $dn/dT = 0.57$ K^{-1}. This value is much larger than $dn/dT \approx 10^{-3}$ for fluids[1] and glasses.[7] This unusually large value of dn/dT makes the transformational thermal pattern very sensitive to all possible heat sources: bulk heating of the sample, laser local heating, and even sample defects. The latter could act as secondary light sources by scattering the incident laser light and produce extra ring patterns.

The temperature dependences of divergence angle θ_c

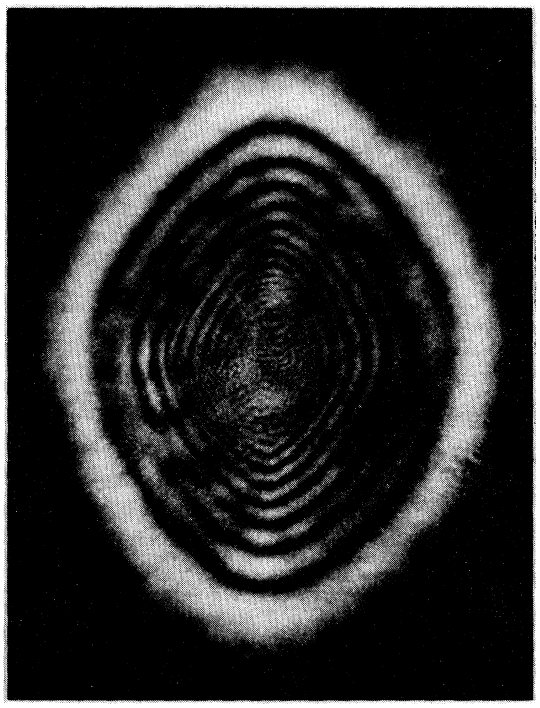

FIG. 7. Far-field thermal-lens pattern near T_c. The radial intensity distribution of the pattern is shown in Fig. 10.

(along the crystal c axis) and θ_a (along the a axis) are plotted in Fig. 8. Double logarithmic plots of θ_c and θ_a versus temperature are shown in Fig. 9, where $T_c = 570.7\,^{\circ}\mathrm{C}$ was taken as the temperature corresponding to the $\theta(T)_{\max}$. The plots shown in Fig. 9 yield $\theta_c \sim \epsilon^{-0.44\pm0.01}$ and $\theta_a \sim \epsilon^{-0.39\pm0.01}$. From Eq. (10) the critical exponent β is obtained as $\beta_c = 0.28\pm0.01$ and $\beta_a = 0.31\pm0.01$, respectively. The advantage of determining the critical exponent according to Eq. (10) is that no other crystal parameters are involved. However, Eqs. (5) and (7), from which Eq. (10) is deduced, are based on a simplified model, in which dn/dT is constant both axially and radially. In fact, dn/dT varies in both directions because of the radial temperature distribution and the absorption of the crystal. This may result in the discrepancy of measured β values from the theoretical expectation of $\frac{1}{4}$. According to the measured β values, we believe that our system is mean field. For a comparison we want to note that $\beta \approx 0.30$ is found for As_2O_5 and attributed to "crossover" behavior.[18]

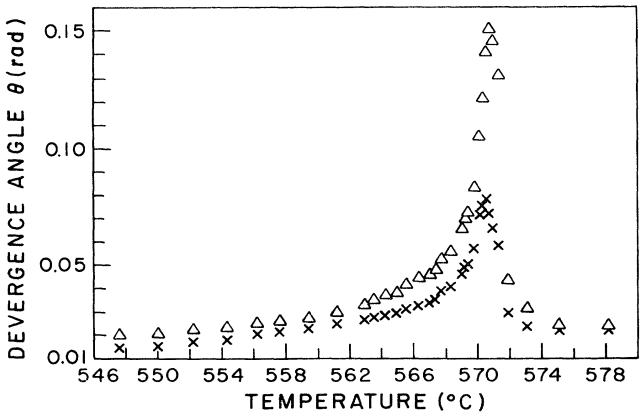

FIG. 8. Temperature dependence of the beam divergence angles θ_c (△) and θ_a (×).

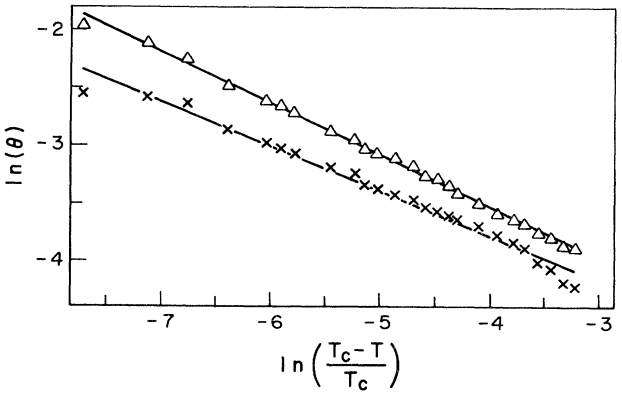

FIG. 9. Double logarithmic plots of the data shown in Fig. 7; the slopes yield $\theta_c \sim \epsilon^{-0.44}$ (△) and $\theta_a \sim \epsilon^{-0.39}$ (×) with $\epsilon = (T_c - T)/T_c$ and $T_c = 570.7\,^{\circ}\mathrm{C}$.

To estimate the self-phase modulation, some quantitative knowledge of the crystal is necessary. For our experiments, with 0.33 W in a $w = 0.213$ mm beam, the maximum value of ΔT is estimated as 0.2 K from Eq. (3). $\Delta n_{\max} = (dn/dT)\Delta T_{\max}$ is, thus, estimated as 0.1. The corresponding phase difference is $\Delta\phi_{\max} \sim 470\pi$.

The intensity distribution of Fig. 7 along the long ellipse axis (parallel to the c axis) is shown in Fig. 10. In comparison with this experimental result, the theoretical illustration of Fig. 5 is basically a good description of the thermal lens pattern, only in Fig. 5 the interference rings distribute intensity mostly in the outer part of the pattern. This inconsistency in intensity distribution is due to the uncertain crystal parameters available and the approximation in which the interfering parts of the beam are considered to reflect at exactly the same angle (i.e., in parallel rays).

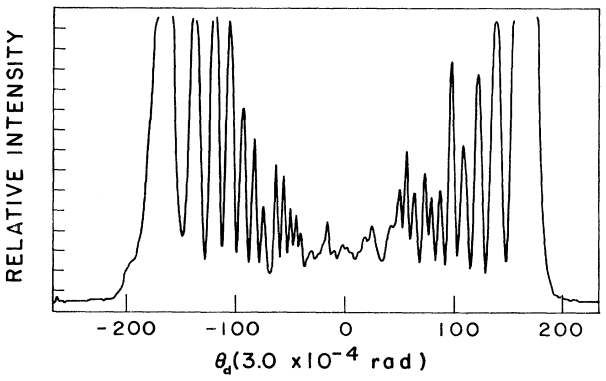

FIG. 10. Intensity distribution of thermal-lens pattern along the c axis. This is an experimental plot of the pattern shown in Fig. 7.

We want to stress that our far-field patterns basically originate from the self-phase modulation of the thermal lens rather than from the Fresnel diffraction, which is of the form of a Bessel-function integral, as in Refs. 6 and 7. Thus, our intensity pattern has a radial distribution that is not a nth-order Bessel function. Basically, Ref. 6 declined to calculate the intensity pattern in the rings, because this required computer calculations not readily available to them. Reference 7 did such a calculation, but, we believe, in the wrong limit; the results of Ref. 7 in the Bessel-function limit are inappropriate for the scattering angle $\geq 4°$ observed in the present work.

ACKNOWLEDGMENTS

This work was supported by Army Research Organization Grant No. DAAL-0390-G0002.

APPENDIX A: DISCUSSION OF THE THEORY OF AKHMANOV *et al.* AND DABBY *et al.*

The only paper dealing with the intensity distribution of the thermal-lens pattern is by Dabby *et al.*[7] They used directly the results by Akhmanov *et al.*[6]

$$I(\theta)=I_0\left|\int_0^a rJ_0(k\theta r)\exp\left[-\frac{r^2}{w_0^2}-ik\left[\frac{r^2}{2R_0}+\frac{r^2}{2z}+\int_0^L \delta n(r,z)dz\right]\right]dr\right|^2 , \tag{A1}$$

with θ as the deflection angle and J_0 the Bessel function of zero order. [Reference 4 stops at Eq. (A1), saying only that it converts a Gaussian input beam into an output consisting of rings described by Airy functions.] For the origin of the Bessel function, we cite here the phase part of diffraction integral from Born and Wolf:[21]

$$U(P)\sim\int_0^1\int_0^{2\pi} e^{i[k\Phi-v\rho\cos(\alpha-\psi)-(1/2)u\rho^2]}\rho\,d\rho\,d\alpha , \tag{A2}$$

where $k\Phi$ is the phase shift from a Gaussian reference sphere to the wave front at the diffraction aperture, while u, v, ρ, α, and ψ are coordinates concerning the diffraction of the reference sphere; $\Phi(r)=\int_0^L \delta n(r,z)dz$. If Φ is α independent, the angular integral in Eq. (2) can be separated and written as a Bessel function:

$$J_0(v\rho)=\frac{1}{2\pi}\int_0^{2\pi} e^{-iv\rho\cos(\alpha-\psi)}d\alpha . \tag{A3}$$

Thus, the Bessel functional rises from the phase shift due to the geometry of the diffraction aperture. $v\rho$ in Eq. (A3) is equivalent to $k\theta r$ in Eq. (A1). Referring to Fig. 11, the other terms in Eq. (A1) are the following: e^{-r^2/w_0^2}, which describes the intensity distribution of a Gaussian beam; $r^2/2R_0=PP'-R_0$, the phase retardation at the input plane of the sample with R_0 as the input beam radius; $r^2/2z=P\tilde{}P'-z$, the phase retardation from the output plane of the sample to the observation plane with z as the distance from the sample to the observation plane. In our experiment, $r\approx 10w_0\approx 2$ mm, $R_0\approx 1000$ mm, $z\approx 2000$ mm. Therefore, the phase shift is mainly due to the difference in optical path length inside the sample.

Akhmanov *et al.* and Dabby *et al.* concluded that J_0 is responsible for the angular structure in the far field. However, in our experiment this is *not true*. We failed to produce a pattern according to Eq. (A1). Now the question is what approximation has been made in deducing Eq. (A1) and whether this approximation is appropriate for our thermal-lens problems. In general, due to the aberration of an optic element, the wave front is deformed after passing through it. For the $Ba_2NaNb_5O_{15}$ thermal lens, the difference in refractive index between beam center $r=0$ and $r=3w_0$ is estimated as approximately 0.1. In this case the wave-front deformation is no longer small. (See Appendix B.) In Fig. 12, σ represents the wave front whose center is directly outside the sample. σ' represents a Gaussian reference sphere. Now, when we consider P's contribution to different points on the observation plane, say, points $P_1\tilde{}, P_2\tilde{}, \ldots$, the optical path differences in Eq. (A2), $\Phi_1, \Phi_2, \ldots$, are no longer equal to a same quantity $P''P'''=\Phi(r)$. The difference in Φ could be much greater than that due to the geometry of the diffraction aperture. Mathematically, because $\Phi=\Phi(\alpha,\psi,P\tilde{})$, Φ is not independent of α and hence the solution to Eq. (A2) is not a Bessel-function product. When the deformation of wave front σ is small enough that $\Phi_1=\Phi_2=\cdots=\Phi(r)$, then Fig. 12 can be simplified to Fig. 11 and the output from the sample is a plane wave with a phase distribution $\Phi(r)$ on it. This phase retardation distribution becomes a modulation to the Bessel function.

In our numerical calculation of Eq. (A1), k and r are determined by the experimental setup. Only when θ is chosen to satisfy $k\theta r<1$, i.e., the modulation occurs in-

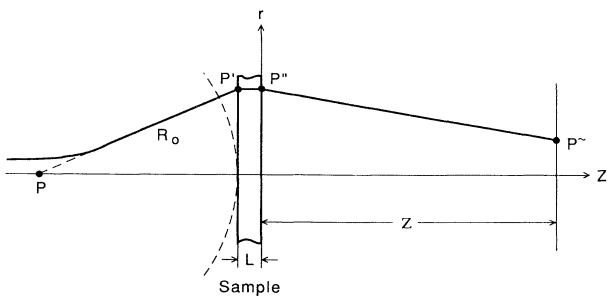

FIG. 11. Schematic illustration of a Gaussian beam propagating through a thermo-optic sample, according to the model in Ref. 7.

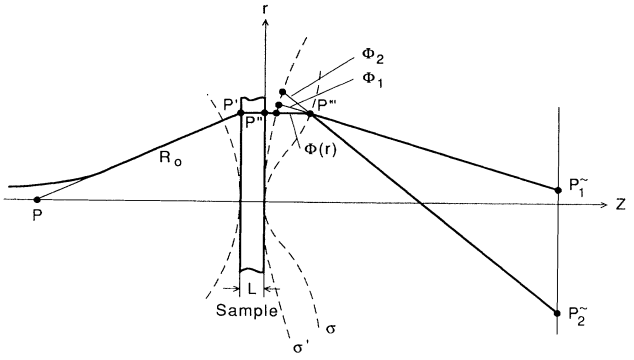

FIG. 12. Schematic illustration of a Gaussian beam propagating through a thermo-optic sample. The wave-front deformation is taken into account: σ, the deformed output wave front; σ', a Gaussian reference sphere.

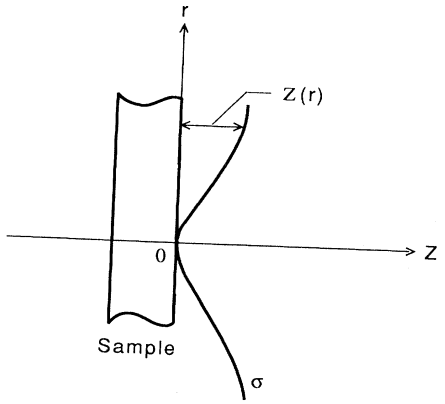

FIG. 13. Estimated wave-front deformation of a Gaussian beam passing through a SBN sample near T_c.

side the first maximum (Airy disc), and when the tail of the Bessel function is cut off, can we obtain a fringe with higher intensity in its outside ring, just as the numerical results in the paper of Dabby *et al.* However, if these conditions are not satisfied, our numerical calculation shows that the phase shift due to a thermal lens is not able to compensate the rapid decay in amplitude of the Bessel function and a thermal-lens fringe cannot be produced by Eq. (A1).

We want to remind readers that Fig. 1(c) of Ref. 7 is obviously not a digital reproduction of Fig. 1(a). From their data, $\theta \simeq 0.06°$. $k_0 \theta r$ is estimated as $\simeq 20\pi$. Their observation of Fig. 1(a) and other observations for liquid media are not in the Bessel-function limit. For $Ba_2NaNb_5O_{15}$ near T_c, we estimate $k\theta \approx 10^3$. It is even further beyond the region in which a Bessel function presents its structure.

An accurate calculation of the thermal-lens diffraction can be carried out either based on the wave model in Fig. 12 or on a light ray approach. For the former, the deformed wave front is the source of the secondary wavelet and we need to find an expression of Φ. As to the latter, the wave-front deformation is treated as a beam deflection in an inhomogeneous medium. In our present paper we calculate first the beam deflection and then the interference of two parts of the beam according to their phase difference. This approximation is still rough, but it includes the basic features of the phase modulation of the thermal lens. Our numerical results are in good agreement with the experimental observations.

APPENDIX B: ESTIMATION OF THE WAVE-FRONT DEFORMATION

Referring to Fig. 13, the time required for light traveling through the sample at its polar coordinate r is

$$t(r)=\frac{L}{c}n(r) ,$$
$$\Delta t(r)=t(0)-t(r)=\frac{L}{c}[n(0)-n(r)] . \tag{B1}$$

Here we ignore the beam deflection inside the sample. At the moment when the beam center just passes the sample,

$$z(0)=0 ,$$
$$z(r)=c\Delta t=L[n(0)-n(r)] . \tag{B2}$$

The numerical calculation shows that the temperature increment ΔT occurs mostly in $r \leq 3w_0$. That is,

$$z(3w_0 \approx 0.6 \text{ mm})=(1.3 \text{ mm})(0.1)=0.13 \text{ mm} .$$

*Permanent address: Department of Physics, Nankai University, Tianjin, China.

[1]J. P. Gordon, R. C. C. Leite, R. S. Moore, S. P. S. Porto, and J. R. Whinnery, J. Appl. Phys. **36**, 3 (1965).
[2]J. F. Scott, S.-J. Sheih, K. R. Furer, N. A. Clark, W. F. Oliver, and S. A. Lee, Phys. Rev. B **41**, 9330 (1990).
[3]J. F. Scott, S.-J. Sheih, and T. Chen, Ferroelectrics (to be published).
[4]J. Seglins, A. Krumins, A. Ozols, and S. Odoulov, Ferroelectrics **75**, 317 (1987).
[5]A. Krumins, A. Anspoks, S. G. Odoulov, J. Seglines, and P. Vaidods, Ferroelectrics **80**, 277 (1988).
[6]S. A. Akhmanov, D. P. Krindach, A. P. Sukhorukov, and R. V. Khokhlov, Pis'ma Zh. Eksp. Teor. Fiz. **6**, 509 (1967) [JETP Lett. **6**, 38 (1967)].
[7]F. W. Dabby, T. K. Gustafson, J. R. Whinnery, Y. Kohanzadeh, and P. L. Kelley, Appl. Phys. Lett. **16**, 362 (1970).
[8]W. R. Cullen, B. G. Huth, and R. H. Pantell, Appl. Phys. Lett. **11**, 103 (1967).
[9]J. R. Whinnery, D. T. Miller, and F. W. Dabby, J. Quantum Electron. **QE-3**, 382 (1967).
[10]H. Inaba and H. Ito, J. Quantum Electron. **QE-4**, 45 (1968).
[11]S. A. Akhmanov, D. P. Krindach, A. V. Migulin, A. P. Sukhorukov, and R. V. Khokhlov, J. Quantum Electron.

QE-4, 568 (1968); S. A. Akhmanov, A. P. Sukhorukov, and R. V. Khokhlov, Zh. Eksp. Teor. Fiz. **50**, 1537 (1966) [Sov. Phys. JETP **23**, 1025 (1966)].

[12]J. H. Wenderoff and M. Eich, Mol. Cryst. Liq. Cryst. **169**, 133 (1989).

[13]J. S. Abell, K. G. Barraclough, I. R. Harris, A. W. Vere, and B. J. Cockayne, Mater. Sci. **6**, 1084 (1971).

[14]S. J. Sheldon, L. V. Knight, and J. M. Thome, Appl. Opt. **21**, 1663 (1982).

[15]Tomoaki Yamada, Hiroshi Iwasaki, and Nobukazu Niizeki, J. Appl. Phys. **41**, 4141 (1970).

[16]S. Singh, D. A. Draegert, and J. E. Geusic, Phys. Rev. B **2**, 2709 (1970).

[17]M. E. Lines and A. M. Glass, *Principles and Applications of Ferroelectric and Related Materials* (Clarendon, Oxford, 1977), p. 480.

[18]E. Salje, U. Bismayer, and M. Jansen, J. Phys. C **20**, 3613 (1987).

[19]M. DiDomenico, Jr. and S. H. Wemple, J. Appl. Phys. **40**, 720 (1969).

[20]G. H. Burkhart and R. R. Rice, J. Appl. Phys. **48**, 4817 (1977).

[21]M. Born and E. Wolf, *Principles of Optics* (Pergamon, New York, 1959), p. 460.

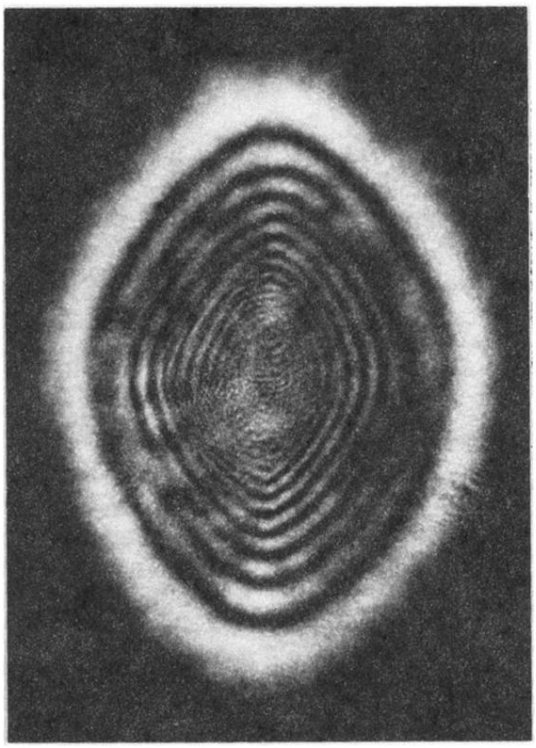

FIG. 7. Far-field thermal-lens pattern near T_c. The radial intensity distribution of the pattern is shown in Fig. 10.